JACS
JOURNAL OF THE AMERICAN CHEMICAL SOCIETY

ARTICLE

pubs.acs.org/JACS

Development of a Highly Sensitive Fluorescence Probe for Hydrogen Peroxide

Masahiro Abo,[†,§] Yasuteru Urano,[‡] Kenjiro Hanaoka,[†,§] Takuya Terai,[†,§] Toru Komatsu,[†,§] and Tetsuo Nagano*[,†,§]

[†]Graduate School of Pharmaceutical Sciences, The University of Tokyo, 7-3-1 Hongo, Bunkyo-ku, Tokyo 113-0033, Japan

[‡]Graduate School of Medicine, The University of Tokyo, 7-3-1 Hongo, Bunkyo-ku, Tokyo 113-0033, Japan

[§]CREST, JST, Sanbancho-blg, 5 Sanbancho, Chiyoda-ku, Tokyo, 102-0075, Japan

Supporting Information

ABSTRACT: Hydrogen peroxide is believed to play a role in cellular signal transduction by reversible oxidation of proteins. Here, we report the design and synthesis of a novel fluorescence probe for hydrogen peroxide, utilizing a photoinduced electron transfer strategy based on benzil chemistry to control the fluorescence. The practical value of this highly sensitive and selective fluorescence probe, NBzF, was confirmed by its application to imaging of hydrogen peroxide generation in live RAW 264.7 macrophages. NBzF was also employed for live cell imaging of hydrogen peroxide generated as a signaling molecule in A431 human epidermoid carcinoma cells.

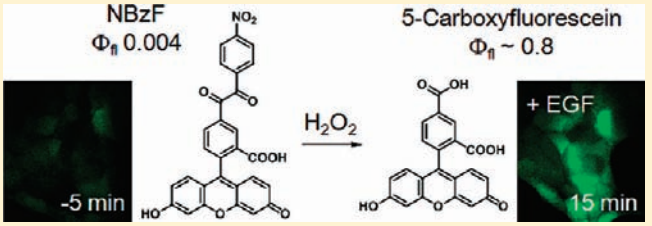

INTRODUCTION

Reactive oxygen species (ROS) are a class of radical or nonradical oxygen-containing molecules that show high reactivity to biomolecules.[1] Excessive ROS generation is involved in the pathogenesis of many diseases, including cardiovascular disease,[2] cancer,[3] and neurological disorders.[4] However, the physiological level of ROS is believed to be indispensable in regulating diverse cellular processes, such as an immune response[5] and cell signaling.[6] Although generation of ROS is often simply regarded as representing oxidative stress, each ROS has unique chemical characteristics in terms of chemical reactivity and lifetime in aqueous solution and, therefore, may play a distinct role in biological systems.[7] Hydrogen peroxide (H_2O_2) exhibits relatively mild reactivity among ROS and has attracted intense interest recently, because it appears to be involved in signal transduction by reversible oxidation of proteins, such as phosphatases and thioredoxins, in a tightly regulated manner.[8−11] For example, Capasso et al. reported that oxidative inhibition of tyrosine phosphatase SHP-1 is required for the activation of B cells through a B cell antigen receptor *in vivo*.[9] Sensitive and selective detection methods for hydrogen peroxide should be powerful tools for studying such biological phenomena.

Fluorescence sensor probes have been widely used for detecting ROS in living cells. For example, reduced fluorescent dyes such as dichlorodihydrofluorescein are commonly used as fluorescence probes for ROS. However, they have critical drawbacks for selective sensing of hydrogen peroxide; namely, they are nonspecific among ROS and also undergo autoxidation upon light irradiation.[12] On the other hand, some fluorescence probes specific for hydrogen peroxide have been reported, based on benzenesulfonyl ester or boronate ester chemistry,[13−15] but their reaction rates and fluorescence background levels are generally not satisfactory for biological applications.[16] These probes are also reported to show a fluorescence increment when they are exposed to nitric oxide, in addition to hydrogen peroxide. In this manuscript, we describe a new type of fluorescence probe with high sensitivity and selectivity for hydrogen peroxide, developed by utilizing the chemical properties of benzil (α-dibenzoyl) in combination with one of our rational probe design strategies, i.e., photoinduced electron transfer (PeT).[17]

As a reactive moiety for hydrogen peroxide, we focused on benzil, because it has unique reactivity with hydrogen peroxide. Sawaki et al. have reported that benzil is transformed to benzoic anhydride through a Baeyer−Villiger type reaction with hydrogen peroxide in alkaline organic solvents, and this is followed by hydrolysis to give benzoic acid (Scheme 1).[18] Though the reported conditions were far from biological in terms of basicity, solvents, and concentration of reagents, we expected that the reactivity between benzil and hydrogen peroxide could be adjusted by modification of the benzene ring of benzil. At the same time, we chose the photoinduced electron transfer mechanism as a strategy for controlling fluorescence, among various possible mechanisms, for the following reasons. We found by means of cyclic voltammetry that benzil has a high reduction potential of no less than −1.1 V vs SCE in acetonitrile. We previously examined the relationship between the fluorescence quantum efficiency of fluorescein derivatives and the reduction potential of the fluorescein benzene moiety and found that fluorescein derivatives whose benzene moiety has a higher reduction potential than −1.8 V vs SCE show almost no fluorescence owing to

Received: April 17, 2011
Published: June 21, 2011

dx.doi.org/10.1021/ja203521e | *J. Am. Chem. Soc.* 2011, 133, 10629–10637

Scheme 1. Proposed Reaction Mechanism between Benzil and Hydrogen Peroxide

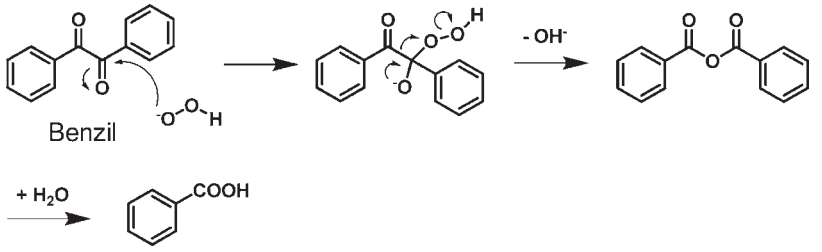

Scheme 2. Design of Fluorescence Probes for Hydrogen Peroxide

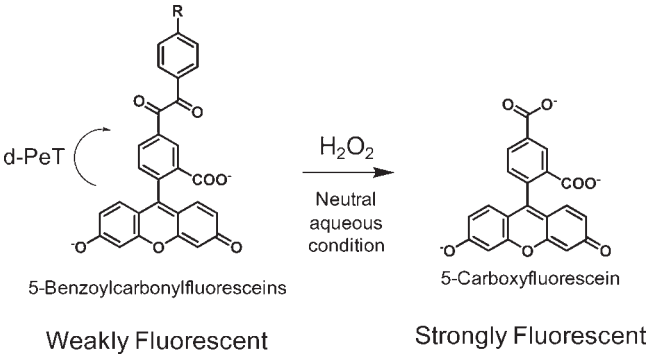

fluorescence quenching through the donor-excited photoinduced electron transfer (d-PeT) process.[19] The high reduction potential of benzil indicates that benzil has a low enough LUMO energy level to accept an electron from an excited fluorophore and, thus, should work as a fluorescence quenching moiety in the d-PeT process, if it is located sufficiently close to the fluorophore. As a fluorophore scaffold, we selected fluorescein, which is widely used for fluorescence bioimaging because of its biocompatibility and excellent photochemical properties, such as excitation and emission wavelengths in the visible region and high fluorescence quantum efficiency.[20,21] Thus, we designed 5-benzoylcarbonylfluorescein derivatives as candidate fluorescence probes for hydrogen peroxide (Scheme 2). The design is based on the idea that these molecules have low fluorescence quantum efficiency, owing to quenching of fluorescence via the intramolecular d-PeT process, before reaction with hydrogen peroxide, but are converted to 5-carboxyfluorescein, which is highly fluorescent, by reaction with hydrogen peroxide.

RESULTS AND DISCUSSION

Synthesis and Photochemical Properties of 5-Benzoylcarbonylfluoresceins. We synthesized five derivatives with various electron-donating or -withdrawing substituents on the benzil moiety (Scheme 3). All of them showed similar photochemical properties to those of fluorescein, except for low fluorescence quantum efficiency owing to efficient quenching via the d-PeT process (Table 1). Among these compounds, NBzF showed extremely weak fluorescence owing to the presence of the nitro group, which lowers the LUMO energy level of benzil, and it is considered that the background fluorescence due to unreacted molecules would be sufficiently low to permit effective bioimaging.

Evaluation of the Response to Hydrogen Peroxide and Other Reactive Oxygen Species *in Vitro*. At the beginning of our investigation, we synthesized 5-benzoylcarbonylfluorescein (**1**) and evaluated its reactivity with hydrogen peroxide by measuring the fluorescence increment after the reaction. Compound **1** showed a small fluorescence increment after incubation with 100 μM hydrogen peroxide for 1 h in 0.1 M sodium phosphate buffer at pH 7.4 (Figure 1). We considered this result to be promising because it indicated that the reaction of benzil and hydrogen peroxide could occur under physiological conditions. However, the reactivity of **1** was rather low and further optimization was needed to obtain a compound exhibiting sufficient reactivity with hydrogen peroxide to be practically usable in biological systems. For this purpose, we synthesized derivatives with various electron-donating or -withdrawing substituents and evaluated them under the same conditions as those used for **1**. Compound **2**, which has a moderately electron-withdrawing substituent, bromine, showed a larger fluorescence increment than **1**. On the other hand, compound **3** with an electron-donating methoxy group showed almost no fluorescence increment under these conditions. These results led us to introduce strongly electron-withdrawing substituents, such as cyano and nitro groups, into benzil. Finally, we found that derivatives with strongly electron-withdrawing groups, compound **4** with a cyano group and NBzF with a nitro group, showed a very large fluorescence increment. Further evaluation was performed with these two compounds. Compound **4** and NBzF showed a rapid fluorescence increase even at low concentrations of hydrogen peroxide (Figure 2). By fitting the data with a pseudo-first-order model (1 μM dye and 1 mM hydrogen peroxide), the reaction rate constants were obtained as 3.4×10^{-3} s^{-1} and 4.2×10^{-3} s^{-1} for **4** and NBzF, respectively, at 37 °C (Table 2). These values are comparable to those of previously reported fluorescence probes for hydrogen peroxide based on boronate chemistry.[15] Though the reactivities of **4** and NBzF with hydrogen peroxide were almost the same, NBzF showed a much higher signal-to-noise ratio than did **4**, because of its extremely low fluorescence quantum efficiency before reaction with hydrogen peroxide. Indeed, the enhancement of fluorescence intensity after reaction with hydrogen peroxide was as high as 150-fold (Figure 3). This fluorescence enhancement ratio is superior to that of any previously reported fluorescence probe for hydrogen peroxide. For example, two boronate-based fluorescence probes for hydrogen peroxide, Peroxy Crimson 1 and Peroxyfluor-3, are reported to show approximately 40-fold fluorescence enhancement upon addition of hydrogen peroxide.[14,15] The generation of 5-carboxyfluorescein after the reaction of NBzF with hydrogen peroxide was also confirmed by HPLC analysis (Figure 4). Furthermore, we monitored the conversion of NBzF to 5-carboxyfluorescein (5-CF) and 4-nitrobenzoic acid (4-NO_2BA) upon reaction with

Scheme 3. Synthesis of 5-Benzoylcarbonylfluorescein Derivatives[a]

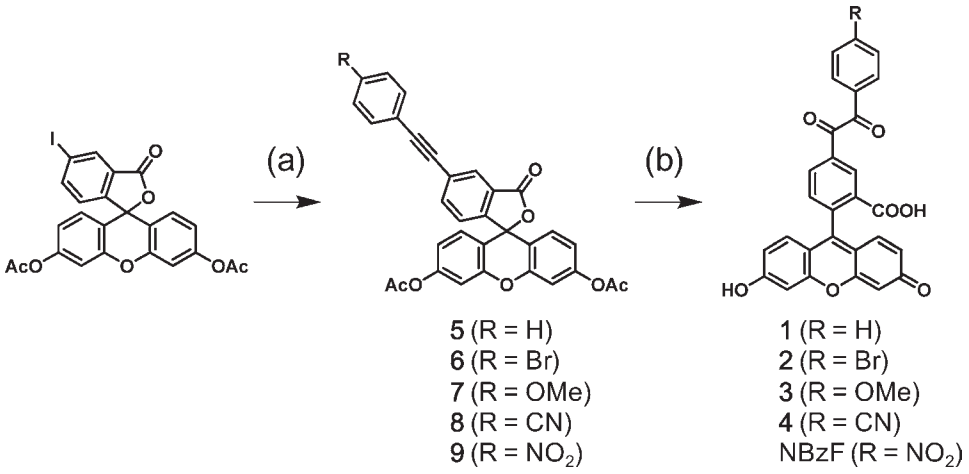

[a] Reagents and conditions: (a) ethynylbenzenes, $PdCl_2(PPh_3)_2$, triethylamine, THF; (b) (i) $PdCl_2$, DMSO, (ii) K_2CO_3, MeOH for **1**−**4** or (i) K_2CO_3, MeOH (ii) $PdCl_2$, DMSO for NBzF.

Table 1. Photochemical Properties of 1−4 and NBzF in 0.1 M Sodium Phosphate Buffer at pH 7.4

Compound	Absorbance max (nm)	Extinction coefficient ε (M^{-1} cm^{-1})	Emission max (nm)	Fluorescence quantum efficiency Φ_{fl}
1	494	7.8×10^4	520	0.023
2	493	7.8×10^4	518	0.022
3	494	6.9×10^4	518	0.026
4	493	7.2×10^4	518	0.060
NBzF	495	6.8×10^4	519	0.004

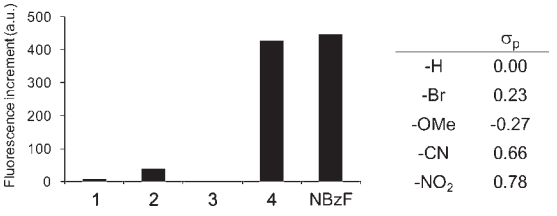

Figure 1. Fluorescence increment of the compounds after reaction with hydrogen peroxide. Compounds (10 μM) were incubated with hydrogen peroxide (100 μM) at 37 °C for 1 h in 0.1 M sodium phosphate buffer at pH 7.4. σ_p is the para substituent constant of the Hammett equation.[22] Fluorescence increase at 520 nm was measured with excitation at 490 nm.

hydrogen peroxide by means of NMR spectroscopy (Figures 5 and S12, Supporting Information). The reaction was performed with 2 mM NBzF and 20 mM hydrogen peroxide in DMSO-d_6 containing 20% 0.1 M sodium phosphate buffer at pH 7.4. No major product other than 5-carboxyfluorescein and 4-nitrobenzoic acid was detected after incubation for 30 min. In the NMR spectra of the reaction mixture, signals of a benzoic anhydride intermediate were not observed at any time point, which indicates that the intermediate would be hydrolyzed immediately under such neutral aqueous conditions. We further examined the reactivity of NBzF toward various ROS by means of fluorescence spectrometry (Figure 6). NBzF did not show any fluorescence enhancement in response to superoxide ($O_2^{-\bullet}$), hydroxyl radical (•OH), hypochlorite ($^-$OCl), nitric oxide (•NO), or singlet oxygen ($^1O_2$). Small fluorescence enhancements were observed with peroxynitrite ($ONOO^-$) and *tert*-butyl hydroperoxide (TBHP), which afforded 5-carboxyfluorescein as a product (Figure S9, Supporting Information). Compared with previously reported fluorescence probes utilizing benzenesulfonyl ester or boronate ester chemistry, the selectivity of NBzF among ROS is unique, because it is unresponsive to nitric oxide. We also investigated the fluorescence response of compounds **1**−**4** to various ROS (Figure S11, Supporting Information). The selectivity of **4** was similar to that of NBzF; it showed a large fluorescence increment with hydrogen peroxide and small increments with peroxynitrite and *tert*-butyl hydroperoxide. Compared with **4** and NBzF, compound **2** showed small fluorescence increments with hydrogen peroxide and peroxynitrite, exhibiting relatively poor selectivity for hydrogen peroxide. Compounds **1** and **3** showed very small fluorescence changes, regardless of the ROS that was added. Taking the reaction mechanism into account, it is reasonable that the chemical reactivities of peroxynitrite and *tert*-butyl hydroperoxide are similar to that of hydrogen peroxide, because all of them have a hydroperoxide structure. However, the concentration of peroxynitrite in living organisms is thought to be far lower than that of hydrogen peroxide, because peroxynitrite has a very short lifetime under physiological conditions owing to its high reactivity with cellular antioxidants.[7] In the case of the fluorescence increment due to *tert*-butyl hydroperoxide, the rate of 5-carboxyfluorescein formation was approximately 7 times slower than that with hydrogen peroxide. This result indicates that NBzF is potentially responsive to alkyl hydroperoxides present in living organisms, such as lipid hydroperoxides. However, the concentration of lipid hydroperoxides in plasma and erythrocytes of healthy human subjects is reported to be less than 1 μM, and the interference from lipid hydroperoxides at this level of concentration would be minimal.[23] In addition, NBzF may not react readily with lipid hydroperoxides in living cells, because NBzF is distributed mainly in the cytosolic environment owing to its hydrophilic fluorescein scaffold, while alkyl peroxides exist in the hydrophobic membrane environment.[24] Thus, although NBzF showed relatively small fluorescence enhancements in response to peroxynitrite and *tert*-butyl hydroperoxide *in vitro*, we expected that it would have a high selectivity for hydrogen peroxide in living or-

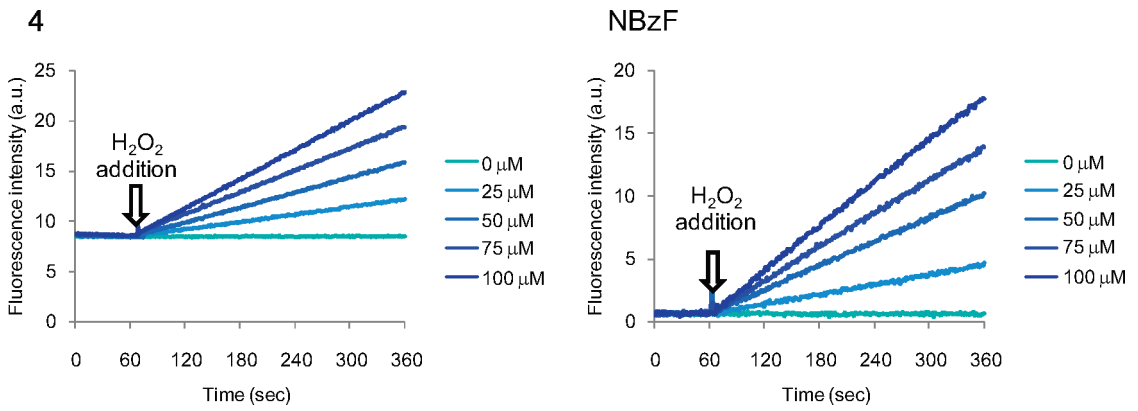

Figure 2. Fluorescence response of **4** and NBzF upon addition of hydrogen peroxide. The indicated concentration of hydrogen peroxide was added at 60 s, and the mixture was incubated at 37 °C in 0.1 M sodium phosphate buffer at pH 7.4. Fluorescence intensity at 520 nm was measured with excitation at 490 nm.

Table 2. Observed Reaction Rate Constants (k) of 4 and NBzF with Hydrogen Peroxide at 25 and 37 °C[a]

	k ($\times 10^{-3}$ s^{-1})	
Compound	25 °C	37 °C
4	1.8	3.4
NBzF	3.2	4.2

[a] The reaction was performed with 1 μM compound and 1 mM hydrogen peroxide in 0.1 M sodium phosphate buffer at pH 7.4.

ganisms. Furthermore, it is possible to distinguish hydrogen peroxide from peroxynitrite by using combinations of inhibitors.

Application of NBzF to Live Cell Imaging Using RAW 264.7 Macrophages. To confirm the practical usefulness of NBzF, we applied diacetylated NBzF (NBzFDA), a membrane-permeable precursor that is hydrolyzed to NBzF by intracellular esterases, for the imaging of hydrogen peroxide generation in living RAW 264.7 macrophages. These macrophages produce superoxide upon stimulation with phorbol-12-myristate-13-acetate (PMA),[25] and it is well-known that superoxide is degraded to hydrogen peroxide by superoxide dismutase or by spontaneous dismutation. In this experiment, RAW 264.7 macrophages were stimulated with 1 μg/mL PMA for 20 min and then loaded with NBzFDA for 20 min. PMA-stimulated RAW 264.7 macrophages formed endosomes, which displayed high levels of fluorescence intensity, while macrophages not stimulated with PMA showed only weak intracellular fluorescence (Figure 7A,B). The fluorescence increment in the endosomes was suppressed by pretreatment with apocynin (5 mM), which is an inhibitor of NADPH oxidase (Nox), or by ebselen (5 μM), which is a mimic of glutathione peroxidase (Figure 7C,D). L-NAME (5 mM), which inhibits the production of nitric oxide by nitric oxide synthase and the subsequent conversion of nitric oxide to peroxynitrite, had little effect on the fluorescence intensity (Figure 7E). Figure 7F shows the averaged fluorescence intensities of the endosomes in the presence or absence of the inhibitors. None of the inhibitors had much influence on the morphological change of the macrophages following PMA stimulation, as judged from bright-field images. Taken together, these results indicate that NBzF is able to visualize endogenous hydrogen peroxide generation in RAW 264.7 macrophages. The background fluorescence was low, and we confirmed that NBzF showed little fluorescence enhancement due to spontaneous decomposition or autoxidation upon light irradiation under the conditions of this experiment.

Live Cell Imaging of Hydrogen Peroxide Generated in A431 Human Epidermoid Carcinoma Cells by Using NBzF. Recently, hydrogen peroxide has emerged as an important signaling molecule for cellular signal transduction following stimulation of cells, e.g., with cytokines, growth factors, and hormones.[26] For example, A431 human epidermoid carcinoma cells are thought to utilize hydrogen peroxide as a signal transducer following epidermal growth factor (EGF) stimulation.[27] It is reported that EGF-stimulated A431 cells transiently generate hydrogen peroxide by activating Nox, leading to inhibition of protein-tyrosine phosphatase 1B by reversible oxidation of the protein and thus strengthening the phosphorylation signal from the EGF receptor.[28] So, we investigated whether NBzF could enable visualization of hydrogen peroxide generated as a signaling molecule in A431 cells. Cultured A431 cells were stained with 5 μM NBzFDA for 10 min at 37 °C and then stimulated with 500 ng/mL of EGF. Images were taken for 30 min by conventional fluorescence microscopy. Time-lapse imaging revealed that A431 cells stimulated with EGF showed a rapid intracellular fluorescence increment, within 20 min, while control cells showed only a slight fluorescence change (Figure 8). This time scale of fluorescence increment is consistent with the literature; it was reported that EGF stimulation induces temporary production of hydrogen peroxide in A431 cells.[27] The fluorescence increment was suppressed by inhibitors of Nox and hydrogen peroxide, supporting the idea that NBzF can detect endogenous hydrogen peroxide in A431 cells (Figure 9). The role of hydrogen peroxide as a signaling molecule has recently attracted enormous interest in biological studies. Our present results suggest that fluorescence imaging with NBzF would offer a powerful detection technique for biological investigations of the involvement of hydrogen peroxide in cellular signal transduction, because NBzF has a much higher reactivity toward hydrogen peroxide as compared with dichlorodihydrofluorescein, the most commonly used indicator for ROS, including hydrogen peroxide (Figure S13, Supporting Information).

CONCLUSION

We designed 5-benzoylcarbonylfluorescein derivatives as candidate fluorescence probes for the detection of hydrogen peroxide by utilizing the unique chemical reactivity of benzil and hydrogen peroxide, together with the d-PeT mechanism to control the fluorescence. Among the compounds synthesized, NBzF afforded the highly sensitive detection of hydrogen peroxide, owing to its extremely low background fluorescence, with a

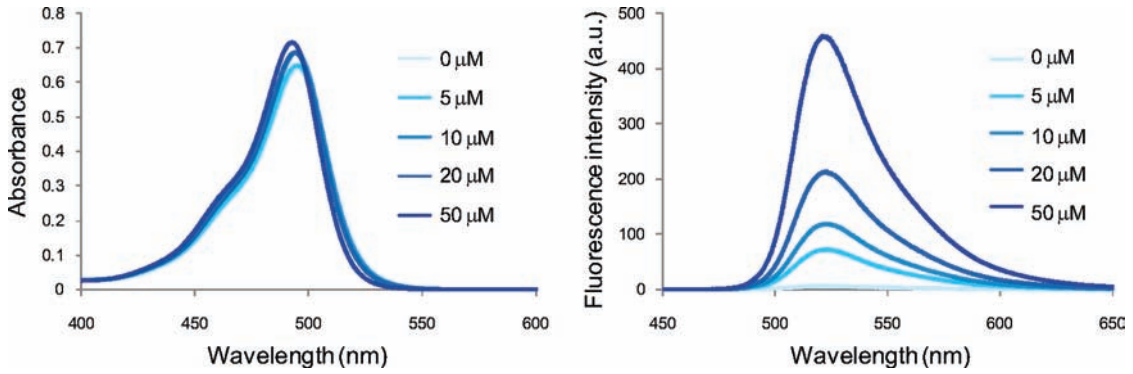

Figure 3. Absorbance and fluorescence spectra of NBzF (10 μM) after incubation with the indicated concentration of hydrogen peroxide. The reaction was performed at 37 °C for 60 min in 0.1 M sodium phosphate buffer at pH 7.4. Fluorescence spectra were measured with excitation at 490 nm.

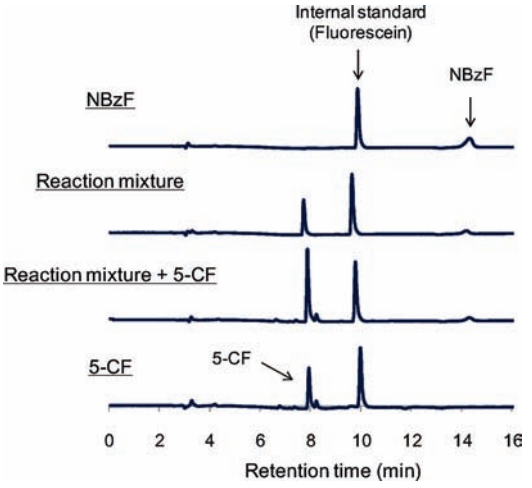

Figure 4. HPLC chromatograms of NBzF (10 μM) before and after reaction with hydrogen peroxide. The reaction was performed with 100 μM hydrogen peroxide at 25 °C for 50 min in 0.1 M sodium phosphate buffer at pH 7.4. The chromatogram of 5-carboxyfluorescein (5-CF, 10 μM) is also shown. Elution was done with a linear gradient (eluent, 0 min, 8% CH_3CN/0.1% TFA aq. ~20 min, 80% CH_3CN/0.1% TFA aq.; flow rate = 1.0 mL/min). Absorbance at 490 nm was detected. Fluorescein was used as an internal standard (peak: 10 min).

good reaction rate and high specificity. We confirmed the practical value of NBzF by using it to detect endogenous hydrogen peroxide generation in living RAW 264.7 macrophages and A431 human epidermoid carcinoma cells. This fluorescence probe offers the highest fluorescence enhancement ratio currently available for hydrogen peroxide detection and should be practically useful as a tool for the study of redox biology. Though indicators for hydrogen peroxide utilizing fluorescent proteins have also been reported,[29] our chemical probe provides an alternative methodology with advantages such as ease of use and high selectivity among ROS. Further, NBzF should be suitable for cell-based high-throughput screening of inhibitors of ROS-producing enzymes, such as NADPH oxidase, providing high screening reliability owing to its high signal-to-noise ratio.[30] The design strategy employed here should be applicable to not only fluorescein derivatives but also other fluorophores, such as rhodamines, boron dipyrromethenes (BODIPYs), and calceins, which would allow control of excitation and emission wavelengths, leakage from cells, and localization to organelles.[31]

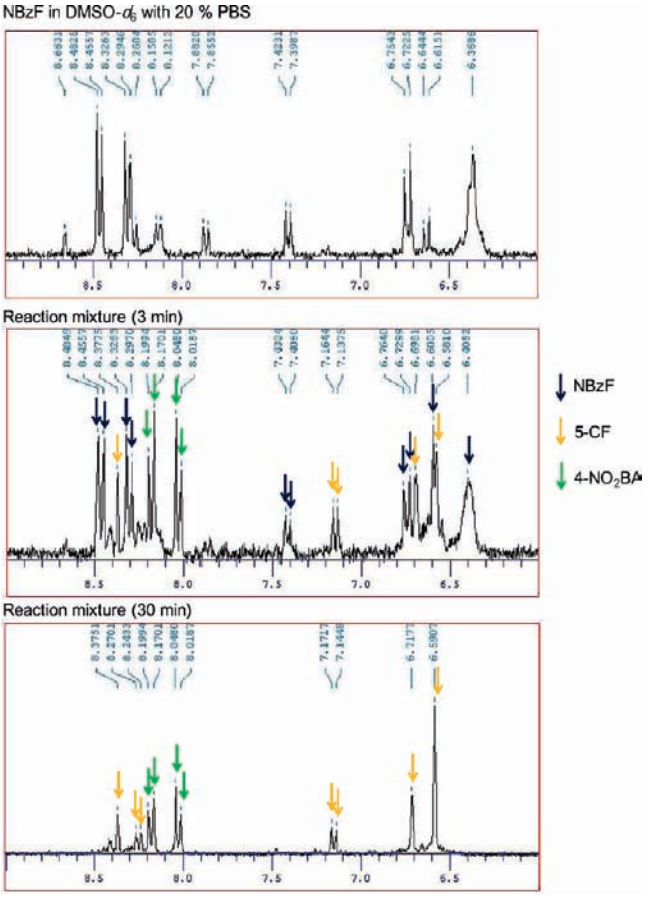

Figure 5. Monitoring of reaction between NBzF and hydrogen peroxide by means of NMR spectroscopy. The reaction was performed with 2 mM NBzF and 20 mM hydrogen peroxide at 25 °C for the indicated time period in DMSO-d_6 containing 20% 0.1 M sodium phosphate buffer (PBS) at pH 7.4.

EXPERIMENTAL SECTION

Materials. General chemicals were of the best grade available, supplied by Tokyo Chemical Industries, Wako Pure Chemical, Daiichi Chemical Co., or Aldrich Chemical Co., and were used without further purification. All solvents were used after appropriate distillation or purification.

Instruments. NMR spectra were recorded on a JEOL JNM-LA300 instrument or a JEOL JNM-LA 400. Mass spectra were measured with a JEOL JMS-T 100LC AccuToF. UV−visible spectra were obtained on a

JASCO V-550. Fluorescence spectroscopic studies were performed on a JASCO FP-6500.

HPLC Analysis. HPLC analysis was performed on an Inertsil ODS-3 column (4.6 mm × 250 mm; GL Sciences Inc.) using an HPLC system composed of a pump (PU-980, JASCO) and a detector (MD-2015 or FP-2025, JASCO). Preparative HPLC was performed on an HPLC system composed of a pump (PU-2080, JASCO) and a detector (MD-2015, JASCO), with an Inertsil ODS-3 column (10.0 mm mm × 250 mm; GL Sciences Inc.).

Fluorometric Analysis. Relative fluorescence quantum efficiencies of dyes were obtained by comparing the area under the emission spectrum of the test sample excited at 490 nm with that of a solution of fluorescein in 0.1 N NaOH, which has a quantum efficiency of 0.85.

Fluorescence Microscopy. Confocal fluorescence imaging studies were performed with a TCS SP5 (Leica Microsystems) equipped with a 63× oil-immersion objective lens and a white-light laser, using a Leica Application Suite Advanced Fluorescence (LAS-AF). NBzF-loaded cells were excited at 495 nm, and emission was collected between 505 and 540 nm. PMT; Gain, 700 V; Offset 0%. Conventional fluorescence images were captured using an Olympus IX 71 equipped with a cooled CCF camera (Coolsnap HQ, Olympus) and a xenon lamp (AH2RX-T, Olympus) with a BP-470-490 excitation filter and a BA-510-550 emission filter.

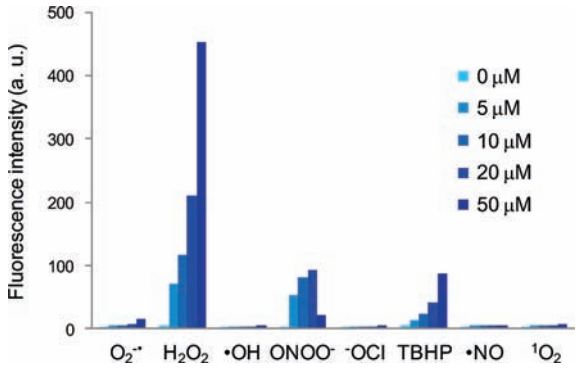

Figure 6. Response of NBzF to various ROS. Fluorescence intensities at 520 nm with excitation at 490 nm are shown. For details; see Figure S1−S8, Supporting Information.

ROS Generating System. The concentration of H_2O_2 was determined from the absorption at 240 nm (ε = 43.6 M^{-1} cm^{-1}). To a solution of dye (10 μM) in 0.1 M sodium phosphate buffer at pH 7.4 containing 0.1% DMF as a cosolvent, H_2O_2 was added at 37 °C, and the spectrum was measured 60 min later. The concentration of $ONOO^-$ was determined from the absorption at 302 nm (ε = 1670 M^{-1} cm^{-1}) in 0.1 N NaOH aq. To a solution of dye (10 μM) in 0.1 M sodium phosphate buffer at pH 7.4 containing 0.1% DMF as a cosolvent, $ONOO^-$ was added at 25 °C, and the spectrum was measured 5 min later. The concentration of ^-OCl was determined from the absorption at 292 nm (ε = 350 M^{-1} cm^{-1}). To a solution of dye (10 μM) in 0.1 M sodium phosphate buffer at pH 7.4 containing 0.1% DMF as a cosolvent, ^-OCl was added at 25 °C, and the spectrum was measured 5 min later. •OH was generated at 25 °C by means of the Fenton reaction with H_2O_2 at the concentration indicated in Figure 2D and a 10-fold excess of $Fe(ClO_4)_2$. *tert*-Butyl hydroperoxide was added at 37 °C to a solution of dye (10 μM) in 0.1 M sodium phosphate buffer at pH 7.4 containing 0.1% DMF as a cosolvent, and the spectrum was measured 60 min later. Nitric oxide was generated from NOC 13 and singlet oxygen was generated from EP-1, which was added at 37 °C to a solution of dye (10 μM) in 0.1 M sodium phosphate buffer at pH 7.4 containing 0.1% DMF as a cosolvent; the spectrum was measured 30 min later.

HPX/Xanthine Oxidase System. Xanthine oxidase (x.o.) from bovine milk, superoxide dismutase (SOD) from bovine erythrocytes, and catalase from bovine liver were purchased from Sigma. Hypoxanthine (HPX) was dissolved in Milli-Q water as a 1.0 mM solution. The generation of superoxide was determined by measuring the reduction of cytochrome *c* (ε_{550} = 19 500 M^{-1} cm^{-1}). HPX was added at 25 °C to a solution of dye (10 μM), xanthine oxidase (23.6 munit/L), and catalase (25 μg protein/mL), and the spectrum was measured 20 min later.

Cell Culture. RAW 264.7 macrophages and A431 cell line were purchased from the RIKEN cell bank. The cells were grown in DMEM (GIBCO) containing 10% heat-inactivated fetal bovine serum (GIBCO), 100 U/mL of penicillin, and 100 μg/mL streptomycin at 37 °C in humidified air containing 5% CO_2.

Live Cell Imaging of RAW 264.7 Cells and Statistical Analysis. RAW 264.7 cells were planted at 5 × 10^4 cells/mL on noncoated glass-bottomed dishes and cultured in DMEM containing 10% heat-inactivated fetal bovine serum (GIBCO), 100 U/mL of penicillin, and 100 μg/mL streptomycin at 37 °C in humidified air containing 5% CO_2 for 2 days. The cells were treated with inhibitors in HBSS for 20 min, activated with

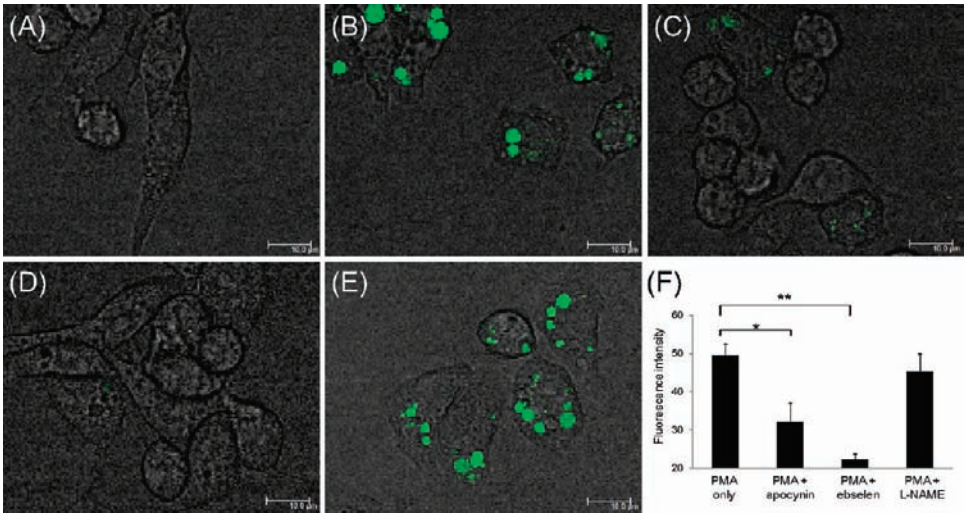

Figure 7. Live cell imaging of RAW 264.7 macrophages stimulated by PMA. RAW 264.7 cells were stimulated for 20 min in the presence or absence of inhibitors, and NBzFDA was loaded for 20 min. (A) Without PMA stimulation. (B) PMA (1 μg/mL) stimulation only. (C) PMA stimulation with 5 mM apocynin. (D) PMA stimulation with 5 μM ebselen. (E) PMA stimulation with 5 mM L-NAME. (F) Fluorescence intensities of endosomes were averaged. Statistical analyses were performed with Student's *t*-test (n = 4). *P < 0.01, **P < 0.001 and error bars are ± s.d.

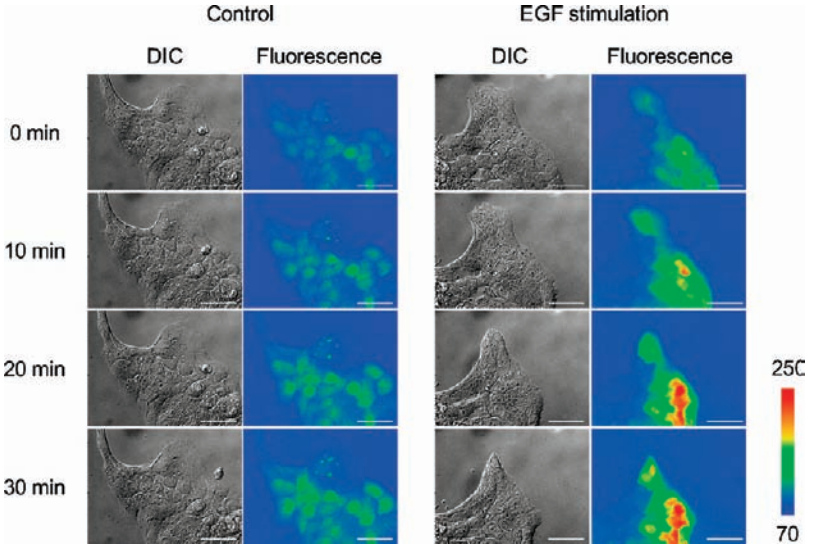

Figure 8. Time-lapse imaging of A431 cells stimulated by EGF. EGF stimulation started at 0 min. Scale bars are 50 μm.

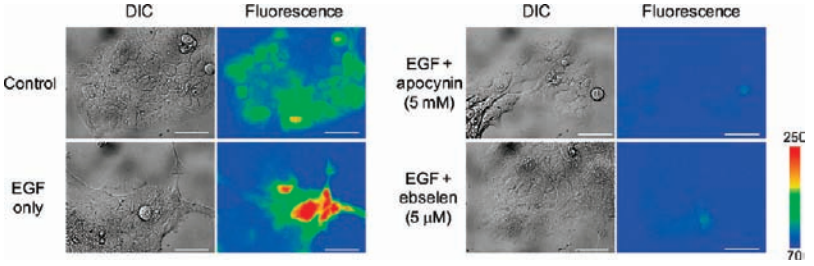

Figure 9. Live cell imaging of A431 cells with inhibitors. NBzFDA (5 μM) and inhibitors were loaded on A431 cells at 37 °C for 10 min, and then cells were stimulated by 500 ng/mL of EGF for 30 min. Scale bars are 50 μm.

1 μg/mL of PMA, and stained with NBzFDA for 20 min at 37 °C in humidified air containing 5% CO_2. The cells were washed by HBSS once, and images were taken. For statistical analysis, fluorescence images were taken every ca. 1 μm along the *z* axis, affording 10 images over each cell body in a field. Fluorescence intensities of endosomes in all 10 images per cell were averaged.

Live Cell Imaging of A431 Cells. A431 cells were plated at 5×10^4 cells/mL on PLL-coated glass-bottomed dishes and cultured in DMEM containing 10% heat-inactivated fetal bovine serum (GIBCO), 100 U/mL of penicillin, and 100 μg/mL streptomycin at 37 °C in humidified air containing 5% CO_2 for 2 days. The cells were cultured in DMEM without FBS for a day before the imaging experiment. The medium was replaced with 2 mL of DPBS containing 0.1 g/L $CaCl_2$ and 0.1 g/L $MgCl_2 \bullet 6H_2O$, and then 5 μM NBzFDA and inhibitor were loaded into the cells at 37 °C for 10 min. Cells were stimulated with 500 ng/mL EGF, and images were taken by conventional microscopy at 37 °C over 30 min.

Synthesis of 5-Iodofluorescein. 5-Iodofluorescein diacetate was prepared by a known method.[32]

Synthesis of 5. 5-Iodofluorescein (206 mg, 0.380 mmol), ethynylbenzene (0.050 mL, 0.455 mmol), $PdCl_2(PPh_3)_2$ (17.5 mg, 0.0250 mmol), and CuI (5.18 mg, 0.0272 mmol) were mixed in 10 mL of dry THF, and 0.25 mL of triethylamine was added. The mixture was stirred at 25 °C for 10 h under an Ar atmosphere. THF was evaporated and the mixture was purified by column chromatography over silica gel using dichloromethane as the eluent, affording the product (150 mg, 76%) as a brown solid. ^{1}H NMR (300 MHz, $CDCl_3$) δ 8.16 (d, 1H, J = 0.73 Hz), 7.81 (dd, 1H, J = 8.07, 1.47 Hz), 7.51 (m, 2H), 7.40 (m, 3H), 7.18 (dd, 1H, J = 7.98, 0.64 Hz), 7.11 (dd, 2H, J = 1.83, 0.73 Hz), 6.84 (m, 4H). ^{13}C NMR (75 MHz, $CDCl_3$) δ 168.8, 168.2, 152.1, 151.5, 138.2, 131.8, 128.9, 128.5, 128.0, 126.6, 125.8, 124.1, 122.3, 117.8, 116.1, 110.5, 91.9, 87.3, 81.8, 76.6, 21.1. HRMS (ESI+) Calcd for [M + H], 517.12873; Found, 517.12477 (−3.95 mmu).

6, **7**, **8**, and **9** were similarly prepared from 4-bromoethynylbenzene, 4-methoxyethynylbenzene, 4-cyanoethynylbenzene, and 4-nitroethynylbenzene in 57%, 91%, 91%, and 78% yield, respectively.

6: ^{1}H NMR (300 MHz, $CDCl_3$) δ 8.15 (dd, 1H, J = 1.47, 0.73 Hz), 7.80 (dd, 1H, J = 7.89, 1.47 Hz) 7.53 (dt, 2H, J = 8.74, 2.11 Hz) 7.42 (dt, 2H, J = 8.74, 2.02 Hz), 7.18 (dd, 1H, J = 8.07, 1.01 Hz), 7.11 (dd, 2H, J = 1.74, 1.01 Hz), 6.83 (m, 4H), 2.32 (s, 6H). ^{13}C NMR (75 MHz, $CDCl_3$) δ 168.6, 168.0, 152.1, 151.4, 138.1, 133.1, 128.8, 127.9, 126.5, 125.3, 124.1, 123.2, 121.1, 117.8, 115.8, 110.4, 90.7, 88.3, 81.6, 21.0. HRMS (ESI+) Calcd for [M + H], 595.03924; Found, 595.03543 (−3.81 mmu).

7: ^{1}H NMR (300 MHz, $CDCl_3$) δ 8.13 (dd, 1H, J = 1.47, 0.72 Hz), 7.78 (dd, 1H, J = 7.86, 1.47 Hz), 7.50 (dd, 2H, J = 6.75, 2.01 Hz), 7.15 (dd, 1H, J = 7.86, 0.54 Hz), 7.10 (dd, 2H, J = 2.01, 0.75 Hz), 6.91 (dd, 2H, J = 6.96, 2.19 Hz), 6.85 (m, 2H), 6.84 (m, 2H), 3.85 (s, 3H), 2.32 (s, 6H). ^{13}C NMR (75 MHz, $CDCl_3$) δ 168.8, 168.3, 160.2, 152.1, 151.6, 151.6, 138.0, 133.3, 128.9, 127.8, 126.6, 126.2, 124.0, 117.8, 116.1, 114.4, 114.2, 110.4, 92.1, 86.2, 81.7, 55.3, 21.1. HRMS (ESI+) Calcd for [M + H], 547.13929; Found, 547.13710 (−2.19 mmu).

8: ^{1}H NMR (300 MHz, $CDCl_3$) δ 8.18 (d, 1H, J = 0.54 Hz), 7.82 (dd, 1H, J = 8.07, 1.47 Hz), 7.68 (d, 2H, J = 7.89 Hz), 7.64 (d, 2H, J = 7.86 Hz), 7.20 (d, 1H, J = 8.04 Hz), 7.11 (m, 2H), 6.84 (m, 4H), 2.32 (s, 6H). ^{13}C NMR (75 MHz, $CDCl_3$) δ 168.7, 168.0, 152.7, 152.2, 151.4, 138.3, 132.2, 132.1, 128.8, 128.3, 127.1, 126.6, 124.7, 124.3, 118.2, 117.8, 115.8,

112.2, 110.5, 91.3, 89.8, 81.8, 21.0. HRMS (ESI+) Calcd for [M + H], 542.12398; Found, 542.12316 (−0.82 mmu).

9: ^{1}H NMR (300 MHz, $CDCl_3$) δ 8.25 (dt, 2H, J = 8.79, 2.11 Hz), 8.20 (dd, 1H, J = 1.28, 0.79 Hz), 7.84 (dd, 1H, J = 8.07, 1.47 Hz), 7.72 (dt, 2H, J = 8.79, 2.11 Hz), 7.22 (dd, 1H, J = 7.98, 0.64 Hz), 7.11 (t, 2H, J = 1.38 Hz), 6.85 (m, 4H). ^{13}C NMR (75 MHz, $CDCl_3$) δ 168.8, 167.9, 152.9, 152.2, 151.5, 147.5, 138.3, 132.5, 129.1, 128.8, 128.4, 126.7, 124.6, 124.4, 123.8, 117.9, 115.8, 110.5, 92.1, 89.6, 81.8, 21.1. HRMS (ESI+) Calcd for [M + Na], 584.09575; Found, 584.09197 (−3.78 mmu).

Synthesis of 1. **5** (51.6 mg, 0.100 mmol) was dissolved in 2 mL of DMSO, and $PdCl_2$ (4.95 mg, 0.0279 mmol) was added to the solution. The reaction mixture was stirred at 105 °C for 12 h under an Ar atmosphere. Then, 2 mL of methanol and K_2CO_3 (100 mg) were added, and the mixture was stirred at 25 °C for 10 min. Purification by preparative HPLC afforded **1** (19.2 mg, 41%) as a yellow solid. ^{1}H NMR (300 MHz, CD_3OD) δ 8.53 (s, 1H), 8.35 (dd, 1H, J = 8.07 Hz), 8.05 (d, 2H, J = 7.70 Hz), 7.76 (t, 1H, J = 7.43 Hz), 7.61 (t, 2H, J = 7.70 Hz), 7.43 (d, 1H, J = 7.89 Hz), 6.73 (d, 2H, J = 2.02 Hz), 6.69 (d, 2H, J = 8.99 Hz), 6.58 (dd, 2H, J = 8.62, 2.20 Hz). ^{13}C NMR (75 MHz, CD_3OD) δ 194.9, 193.9, 169.6, 162.4, 154.5, 136.9, 136.5, 136.0, 134.0, 131.1, 130.5, 130.4, 129.4, 128.1, 127.0, 114.4, 110.9, 103.6. HRMS (ESI−) Calcd for [M − H], 463.08178; Found, 463.07858 (−3.20 mmu).

2, **3**, and **4** were similarly prepared from **6**, **7**, and **8** in 57%, 41%, and 48% yield, respectively.

2: ^{1}H NMR (300 MHz, CD_3OD) δ 8.43 (d, 1H, J = 0.75 Hz), 8.26 (dd, 1H, J = 7.86, 1.47 Hz), 7.87 (d, 2H, J = 8.61 Hz), 7.70 (d, 2H, J = 8.61 Hz), 7.31 (d, 1H, J = 8.04 Hz), 6.60 (d, 2H, J = 2.22 Hz), 6.54 (d, 2H, J = 8.61 Hz), 6.45 (dd, 2H, J = 8.79, 2.40 Hz). ^{13}C NMR (100 MHz, DMSO-d_6) δ 192.1, 191.7, 167.5, 159.8, 157.8, 151.7, 136.4, 133.8, 132.5, 132.0, 131.1, 130.1, 129.3, 127.0, 126.6, 125.3, 112.8, 108.5, 102.3, 83.5. HRMS (ESI−) Calcd for [M − H], 540.99229; Found, 540.98767 (−4.62 mmu).

3: ^{1}H NMR (300 MHz, DMSO-d_6) δ 10.2 (s, 2H), 8.34 (s, 1H), 8.27 (dd, 1H, J = 8.07, 1.29 Hz), 8.00 (d, 2H, J = 8.97 Hz), 7.49 (d, 1H, J = 8.04 Hz), 7.16 (d, 2H, J = 8.79 Hz), 6.70 (d, 2H, J = 2.19 Hz), 6.65 (d, 2H, J = 8.61 Hz), 6.53 (dd, 2H, J = 8.61, 2.19 Hz), 3.89 (s, 3H). ^{13}C NMR (100 MHz, DMSO-d_6) δ 193.0, 192.0, 167.4, 165.18, 159.8, 151.8, 136.1, 134.1, 132.6, 129.3, 127.2, 126.1, 125.4, 124.9, 114.9, 112.7, 108.5, 102.3, 55.9. HRMS (ESI−) Calcd for [M − H], 493.09234; Found, 493.08791 (−4.43 mmu).

4: ^{1}H NMR (300 MHz, DMSO-d_6) δ 10.1 (s, 2H), 8.50 (m, 1H), 8.37 (d, 1H, J = 8.07 Hz), 8.20 (d, 2H, J = 8.25 Hz), 8.10 (d, 2H, J = 8.07 Hz), 7.51 (d, 1H, J = 8.04 Hz), 6.69 (d, 2H, J = 1.65 Hz), 6.63 (d, 2H, J = 8.61 Hz), 6.54 (dd, 2H, J = 8.79, 1.65 Hz). ^{13}C NMR (100 MHz, DMSO-d_6) δ 191.2, 190.7, 167.5, 159.8, 157.8, 151.8, 136.7, 135.5, 133.8, 133.0, 130.8, 129.3, 127.0, 126.9, 125.1, 118.0, 116.8, 112.8, 108.5, 102.3. HRMS (ESI−) Calcd for [M − H], 488.07703; Found, 488.07359 (−3.43 mmu).

Synthesis of NBzF. **9** (58.0 mg, 0.103 mmol) was dissolved in 3 mL of dichloromethane and 3 mL of methanol. Potassium carbonate (62.9 mg, 0.456 mmol) was added. The mixture was stirred at 25 °C for 60 min and then concentrated, and the resulting solid was dissolved in sat. $NaHCO_3$ aq. The water layer was washed with dichloromethane, acidified with 2 N HCl aq., and extracted with ethyl acetate. The organic layer was washed with brine, dried over Na_2SO_4, and concentrated to afford 48.0 mg of an orange solid. The orange solid (19.8 mg) was dissolved in 0.5 mL of DMSO, and $PdCl_2$ (0.72 mg, 4.07 μmol) was added. The mixture was stirred at 145 °C for 4 h under an Ar atmosphere and then purified by preparative HPLC to afford NBzF (10.8 mg, 51%) as a yellow solid. ^{1}H NMR (300 MHz, CD_3OD) δ 8.60 (s, 1H), 8.46 (m, 1H), 8.41 (m, 2H), 8.32 (d, 2H, J = 8.90 Hz), 7.43 (d, 1H, J = 8.04 Hz), 6.70 (d, 2H, J = 2.19 Hz), 6.64 (d, 2H, J = 8.79 Hz), 6.55 (dd, 2H, J = 8.79, 2.19 Hz). ^{13}C NMR (100 MHz, DMSO-d_6) δ 190.7, 190.3, 167.4, 159.7, 157.7, 151.7, 150.8, 136.9, 136.7, 133.8, 131.7, 129.2, 127.0, 126.8, 125.1, 124.0, 112.7, 108.5, 102.3. HRMS(ESI−) Calcd for [M − H], 508.06686; Found, 508.07060 (3.74 mmu).

Synthesis of NBzFDA. **9** (20.1 mg, 0.0358 mmol) was dissolved in 1 mL of DMSO, and $PdCl_2$ (0.65 mg, 3.67 μmol) was added. The mixture was stirred at 145 °C for 4 h under an Ar atmosphere and purified by preparative HPLC to afford NBzFDA (11.0 mg, 52%) as a slightly yellow solid. ^{1}H NMR (300 MHz, DMSO-d_6) δ 8.60 (s, 1H), 8.44 (m, 1H), 8.42 (m, 2H), 8.30 (d, 2H, J = 8.79 Hz), 7.69 (d, 1H, J = 8.04 Hz), 7.32 (d, 2H, J = 1.47 Hz), 7.00 (d, 2H, J = 8.76 Hz), 6.97 (dd, 2H, J = 8.79, 2.22 Hz), 2.30 (s, 6H). ^{13}C NMR (75 MHz, DMSO-d_6) 190.5, 190.2, 168.7, 157.0, 152.3, 150.8, 137.0, 134.2, 131.7, 129.3, 127.3, 126.3, 125.2, 124.0, 118.7, 115.2, 110.6, 81.4, 20.8. HRMS (ESI+) Calcd for [M + Na], 616.08558; Found, 616.08239 (−3.18 mmu).

■ ASSOCIATED CONTENT

Supporting Information. Detailed absorbance and fluorescence changes of NBzF upon addition of various ROS; HPLC analysis of the reaction product of NBzF with various ROS; Fluorescence response of **1**−**4** to various ROS; NMR spectral analysis of the reaction of NBzF and hydrogen peroxide; Kinetic traces of NBzF and hydrogen peroxide; Full information of ref 9. This material is available free of charge via the Internet at http://pubs.acs.org.

■ AUTHOR INFORMATION

Corresponding Author
tlong@mol.f.u-tokyo.ac.jp

■ ACKNOWLEDGMENT

This work was supported in part by a Grant-in-Aid for JSPS Fellows (to M.A.), by a Grant-in-Aid for Specially Promoted Research No. 22000006 to T.N., by the Ministry of Education, Culture, Sports, Science and Technology of Japan (Grant Nos. 19205021 and 20117003 to Y.U., 20689001 and 21659204 to K.H., and 21750135 to T.T.), and by the Industrial Technology Research Grant Program in 2009 for the New Energy and Industrial Technology Development Organization (NEDO) of Japan (to T.T.). K.H. was also supported by the Sankyo Foundation of Life Science.

■ REFERENCES

(1) (a) Finkel, T. *Curr. Opin. Cell Biol.* **2003**, *15*, 247–254. (b) Valko, M.; Leibfritz, D.; Moncol, J.; Cronin, M. T.; Mazur, M.; Telser, J. *Int. J. Biochem. Cell Biol.* **2007**, *39*, 44–84. (c) D'Autreaux, B.; Toledano, M. B. *Nat. Rev. Mol. Cell Biol.* **2007**, *8*, 813–824.

(2) Hansson, G. K.; Libby, P. *Nat. Rev. Immunol.* **2006**, *6*, 508–519.

(3) Seitz, H. K.; Stickel, F. *Nat. Rev. Cancer* **2007**, *7*, 599–612.

(4) Galluzzi, L.; Blomgren, K.; Kroemer, G. *Nat. Rev. Neurosci.* **2009**, *10*, 481–494.

(5) Matsuzawa, A.; Saegusa, K.; Noguchi, T.; Sadamitsu, C.; Nishitoh, H.; Nagai, S.; Koyasu, S.; Matsumoto, K.; Takeda, K.; Ichijo, H. *Nat. Immunol.* **2005**, *6*, 587–592.

(6) Li, Q.; Harraz, M. M.; Zhou, W.; Zhang, L. N.; Ding, W.; Zhang, Y.; Eggleston, T.; Yeaman, C.; Banfi, B.; Engelhardt, J. F. *Mol. Cell. Biol.* **2006**, *26*, 140–154.

(7) Winterbourn, C. C. *Nat. Chem. Biol.* **2008**, *4*, 278–286.

(8) Rhee, S. G. *Science* **2006**, *312*, 1882–1883.

(9) Capasso, M.; et al. *Nat. Immunol.* **2010**, *11*, 265–272.

(10) Funato, Y.; Michiue, T.; Asashima, M.; Miki, H. *Nat. Cell Biol.* **2006**, *8*, 501–508.

(11) Kamata, H.; Honda, S.; Maeda, S.; Chang, L.; Hirata, H.; Karin, M. *Cell* **2005**, *120*, 649–661.

(12) Setsukinai, K.; Urano, Y.; Kakinuma, K.; Majima, H. J.; Nagano, T. *J. Biol. Chem.* **2003**, *278*, 3170–3175.
(13) Maeda, H.; Fukuyasu, Y.; Yoshida, S.; Fukuda, M.; Saeki, K.; Matsuno, H.; Yamauchi, Y.; Yoshida, K.; Hirata, K.; Miyamoto, K. *Angew. Chem., Int. Ed.* **2004**, *43*, 2389–2391.
(14) Miller, E. W.; Tulyathan, O.; Isacoff, E. Y.; Chang, C. J. *Nat. Chem. Biol.* **2007**, *3*, 263–267.
(15) Dickinson, B. C.; Huynh, C.; Chang, C. J. *J. Am. Chem. Soc.* **2010**, *132*, 5906–5915.
(16) Wardman, P. *Free Radical Biol. Med.* **2007**, *43*, 995–1022.
(17) Urano, Y.; Kamiya, M.; Kanda, K.; Ueno, T.; Hirose, K.; Nagano, T. *J. Am. Chem. Soc.* **2005**, *127*, 4888–4894.
(18) Sawaki, Y.; Foote, C. S. *J. Am. Chem. Soc.* **1979**, *101*, 6292–6296.
(19) Ueno, T.; Urano, Y.; Setsukinai, K.; Takakusa, H.; Kojima, H.; Kikuchi, K.; Ohkubo, K.; Fukuzumi, S.; Nagano, T. *J. Am. Chem. Soc.* **2004**, *126*, 14079–14085.
(20) Kojima, H.; Sakurai, K.; Kikuchi, K.; Kawahara, S.; Kirino, Y.; Nagoshi, H.; Hirata, Y.; Nagano, T. *Chem. Pharm. Bull. (Tokyo)* **1998**, *46*, 373–375.
(21) Hirano, T.; Kikuchi, K.; Urano, Y.; Higuchi, T.; Nagano, T. *Angew. Chem., Int. Ed.* **2000**, *39*, 1052–1054.
(22) Hansch, C.; Leo, A.; Taft, R. W. *Chem. Rev.* **1991**, *91*, 165–195.
(23) Niki, E. *Free Radical Biol. Med.* **2009**, *47*, 469–484.
(24) Girotti, A. W. *Free Radical Biol. Med.* **2008**, *44*, 956–968.
(25) Larsen, E. C.; DiGennaro, J. A.; Saito, N.; Mehta, S.; Loegering, D. J.; Mazurkiewicz, J. E.; Lennartz, M. R. *J. Immunol.* **2000**, *165*, 2809–2817.
(26) Brown, D. I.; Griendling, K. K. *Free Radical Biol. Med.* **2009**, *47*, 1239–1253.
(27) Bae, Y. S.; Kang, S. W.; Seo, M. S.; Baines, I. C.; Tekle, E.; Chock, P. B.; Rhee, S. G. *J. Biol. Chem.* **1997**, *272*, 217–221.
(28) Lee, S. R.; Kwon, K. S.; Kim, S. R.; Rhee, S. G. *J. Biol. Chem.* **1998**, *273*, 15366–15372.
(29) Belousov, V. V.; Fradkov, A. F.; Lukyanov, K. A.; Staroverov, D. B.; Shakhbazov, K. S.; Terskikh, A. V.; Lukyanov, S. *Nat. Methods* **2006**, *3*, 281.
(30) Gianni, D.; Taulet, N.; Zhang, H.; Dermardirossian, C.; Kister, J.; Martinez, L.; Roush, W. R.; Brown, S. J.; Bokoch, G. M.; Rosen, H. *ACS Chem. Biol.* **2010**, *5*, 981–993.
(31) (a) Gabe, Y.; Urano, Y.; Kikuchi, K.; Kojima, H.; Nagano, T. *J. Am. Chem. Soc.* **2004**, *126*, 3357–67. (b) Koide, Y.; Urano, Y.; Kenmoku, S.; Kojima, H.; Nagano, T. *J. Am. Chem. Soc.* **2007**, *129*, 10324–10325. (c) Izumi, S.; Urano, Y.; Hanaoka, K.; Terai, T.; Nagano, T. *J. Am. Chem. Soc.* **2009**, *131*, 10189–10200.
(32) Jiao, G. S.; Han, J. W.; Burgess, K. *J. Org. Chem.* **2003**, *68*, 8264.